Desorption yield for valine as induced by fast heavy ions

P. Beining and J. Scheer
Fachbereich 1 (Physik/Elektrotechnik), Universität Bremen, D-2800 Bremen, Federal Republic of Germany

E. Nieschler, B. Nees, and H. Voit
Physikalisches Institut der Universität Erlangen-Nürnberg, D-8520 Erlangen, Federal Republic of Germany
(Received 1 February 1988)

The dependence of the desorption yield for the amino acid valine on the energy of different MeV primary ions has been measured. The primary-ion energies cover a relatively large range with corresponding energy losses between 2 and 55 keV/(μg/cm^2). The observed energy dependence can be understood in the framework of a simple macroscopic model.

I. INTRODUCTION

The desorption of fragile and otherwise involatile molecules by MeV heavy ions, as observed first by Macfarlane and Torgerson,[1] has been the subject of several investigations,[2] which besides the applied aspect had the aim to elucidate the reaction mechanism. The present paper is an extension of previous studies.[3–6] In Ref. 6 we proposed a macroscopic model of the desorption process which could be checked against data from numerous experiments performed for different ions and target substances to study the dependence of the desorption yield on the primary-ion energy. While the energy dependence could be rather well reproduced in all cases, an overall comparison was not yet possible because an overall normalization of the data obtained for different projectiles at different accelerators and different times was lacking. The aim of the present investigation is to obtain a consistent set of data for a number of different projectiles.

II. EXPERIMENTAL PROCEDURE

The Erlanger EN tandem accelerator was used to produce projectiles of ^{12}C (35 MeV), ^{16}O (44 MeV), ^{28}Si (50 MeV), ^{32}S (58 MeV), and ^{65}Cu (60.9 MeV) ions. As described in Refs. 5 and 6, scattering of these projectiles on a thick Pb target produced ions with a continuous energy distribution, which were used to desorb molecules deposited on a thin foil. After passage through this foil the ion energy was measured in a surface barrier detector which also delivered a start signal for a device to register the time of flight of the desorbed molecules. Thus, it was possible to obtain mass spectra of molecules and fragments for different ion energies in a simultaneous measurement. Primary ions with energies smaller than the maximum energy of the recoiling Pb ions were excluded from the measurement. It should be noted that the ions impinging on the desorption target exhibited an equilibrium distribution of charge states.

A crucial point for the kind of measurements performed in this work is the efficiency of the channel plate used to register the desorbed molecules. It depends on the operating mode of the detector. Special care was therefore taken to maintain constant efficiency during the whole experiment in order to get comparable data.

Among the substances investigated in Ref. 6, valine was chosen for comparison with the model predictions, since the set of thermophysical parameters required as input was most complete for this compound. Available parameters refer to *L*-valine, however, while previous experiments[6] were performed with *DL*-valine. To check for possible effects in the present study both *DL*-valine and *L*-valine were investigated.

III. SAMPLE PREPARATION

The amino acid valine (*DL*- and *L*-valine) was deposited on a thin aluminized mylar foil (290 μg cm^{-2} Mylar, 30 μg cm^{-2} Al) by the electrospray method[7] or by vacuum evaporation. The sample thickness was in the order of 30 μg cm^{-2}.

IV. EXPERIMENTAL RESULTS

The measured yields of $[M+\mathrm{H}]^+$ and $[M-\mathrm{H}]^-$ secondary ions desorbed from *L*-valine and *DL*-valine samples are displayed in Figs. 1–3 as a function of the primary-ion energy; $[M+\mathrm{H}]$ and $[M-\mathrm{H}]$ denote the protonated and deprotonated molecular ions, studied in this work.

It should be noted that all yield data were accumulated in one experimental run, i.e., with identically the same experimental setup and the same respective target. Therefore the absolute yield values obtained with different primary ions can be directly compared. It is obvious from Figs. 1–3 that the absolute yields increase with increasing atomic number of the projectile, i.e., with increasing energy loss of the primary ions. The decrease of the yields observed for increasing projectile energy also reflects the dependence on the energy loss. Moreover, the different slopes observed for the yield functions of positive (as well as negative) secondary ions are related with the change of the energy loss occurring in the energy range studied (the energy loss for Cu ions is almost constant whereas that for C ions changes by a factor of 2). Nevertheless, the secondary-ion yield is not proportional

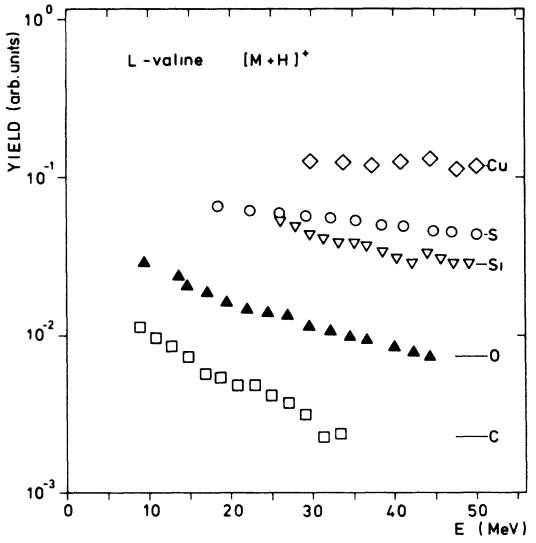

FIG. 1. Yields of $[M+H]^+$ secondary ions from *L*-valine as a function of projectile energy, projectiles as indicated.

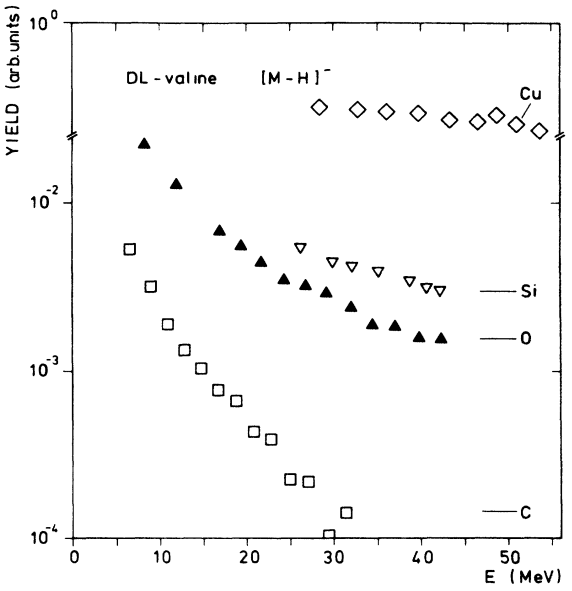

FIG. 3. Yields of $[M-H]^-$ secondary ions from *DL*-valine as a function of projectile energy, projectiles as indicated.

to the energy loss as can be seen from Figs. 4–6, where the yield data of Figs. 1–3 are displayed as a function of the primary-ion energy loss dE/dx, which was calculated according to the Bragg additivity rule from the dE/dx data of Ref. 8. From these figures it is clear the $[M-H]^-$ ions exhibit a much more pronounced dependence on dE/dx than the $[M+H]^+$ ions. Furthermore it should be noted that there may be a threshold for the energy loss to induce desorption, which is emphasized by

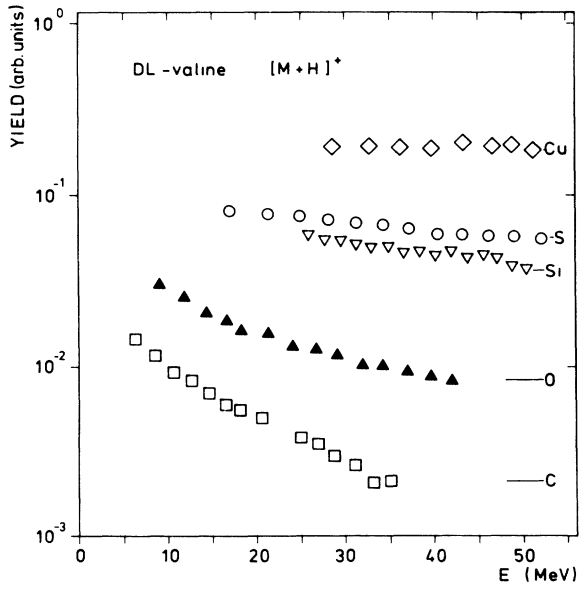

FIG. 2. Yields of $[M+H]^+$ secondary ions from *DL*-valine as a function of projectile energy, projectiles as indicated.

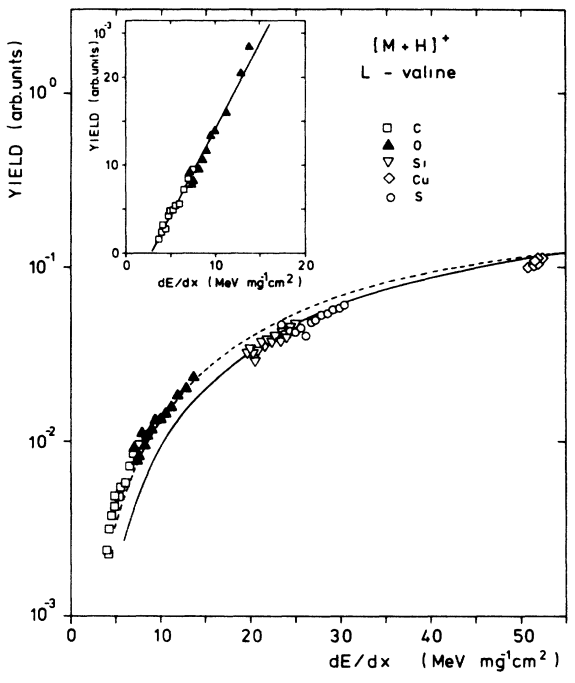

FIG. 4. Yields of $[M+H]^+$ secondary ions from *L*-valine as a function of projectile energy loss, projectiles as indicated. The solid line represents results of model calculations with $U=1.69$ eV, $R_c=10$ Å, and the energy-loss-dependent fragmentation radius R_f from Eq. (3). The dashed line represents results of model calculations with $U=1.19$ eV for the integration parameter $R<30$ Å and $U=1.69$ for $R>30$ Å, and the same parameters R_c and R_f. For details see text. The inset shows the data obtained at small energy losses on a linear scale. The solid line is a guide to the eye.

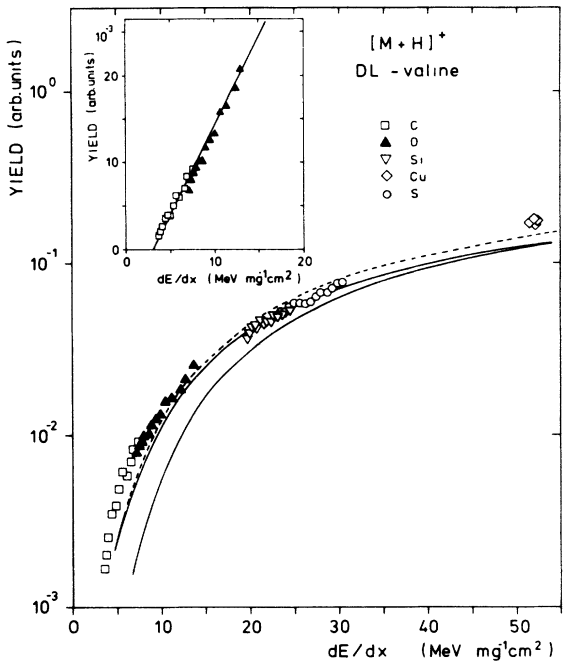

FIG. 5. Yields of $[M+H]^+$ secondary ions from *DL*-valine as a function of projectile energy loss, projectiles as indicated. The lower solid line represents results of model calculations with $U=1.69$ eV, $R_c=30$ Å, $R_f=30$ Å. The upper solid line represents results of model calculations with $U=1.69$ eV, $R_c=10$ Å, and the energy-loss-dependent fragmentation radius R_f from Eq. (3). The dashed line represents results of model calculations with $R_c=R_f=10$ Å. For details see text. The inset shows the data obtained at small energy losses on a linear scale. The solid line is a guide to the eye.

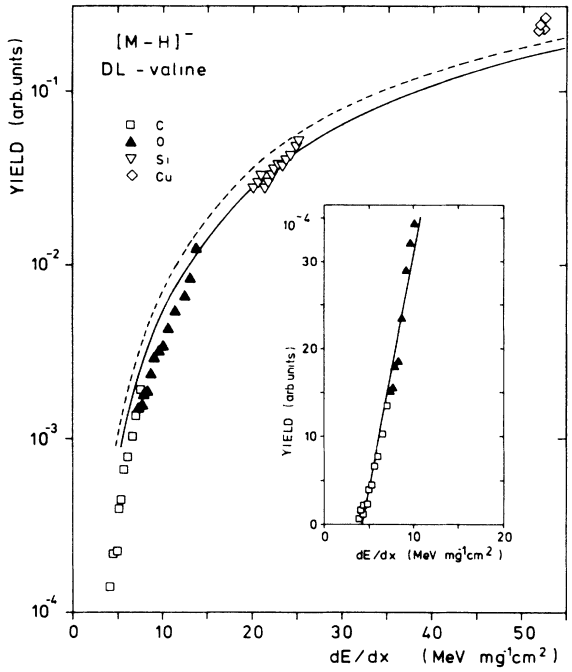

FIG. 6. Yields of $[M-H]^-$ secondary ions from *DL*-valine as a function of projectile energy loss, projectiles as indicated. The solid line represents results of model calculations with $U=4$ eV, $R_c=10$ Å, and the energy-loss-dependent fragmentation radius R_f from Eq. (3). The dashed line represents results of model calculations with $U=3.69$ eV and the same values of R_c and R_f. For details see text. The inset shows the data obtained at small energy loss on a linear scale. The solid line is a guide to the eye.

the linear plots in the insets of Figs. 4–6. This threshold is approximately 3 and 4.2 MeV/mg cm^{-2} for $[M+H]^+$ and $[M-H]^-$ secondary ions, respectively. This observation is in accordance with the results that α particles are not able to desorb molecular ions from a valine sample (see Ref. 9). The maximum energy loss for α particles is 2.3 MeV/mg cm^{-2} in valine.

V. COMPARISON WITH THE MACROSCOPIC MODEL

The basic features of the model, described in detail in Ref. 6, are as follows: It is assumed that desorption takes place only at the very surface, and that the desorption probability is proportional to $e^{-U/E}$, where U denotes an effective binding energy of the surface model and E is that portion of the energy deposited by the primary ion along its parth which reaches the surface at the site of the molecule. There will be a more or less cylindrical region around trajectory of the primary ion which is characterized by a high temperature ("hot core"). The radial extension of this region R_c will be defined by the range of low-energy (<100 eV) electrons which originate from collisions between ion and target electrons and which carry approximately 95% of the deposited energy of the ion, and is of the order of $R_c=10$–40 Å (see Ref. 9). In the model the energy $E(r,t)$ available at the time t at a surface point with distance r from the primary ion trajectory is calculated according to an expression given by Mozumder[10]

$$E(r,t)=kT\left[1+\frac{4\delta t}{R_c^2}\right]^{-1}\exp\left[\frac{-r^2}{R_c^2+4\delta t}\right]. \quad (1)$$

Summing up all times t, all distances r and all annular zones on the sample surface with R, $R+\Delta R$ one obtains a quantity which is proportional to the desorption yield Y.

$$Y\propto\sum_i\sum_j\sum_k R_i\Delta R_j\exp\left[\frac{-u}{E(r_i^k,t_j)}\right], \quad (2)$$

where $T=L/\pi\rho c_v R_c^3$ is the effective temperature of the hot core. It is related to the linear energy tansfer L. The quantities k, δ, ρ, and C_v are the Boltzmann factor, the thermal diffusivity, the density, and the specific heat (at constant volume) of the sample material. The diffusivity is connected with the thermal conductivity κ by $\delta=\kappa/\rho C_v$.

While for desorption of *atomic* ions the sum had to be performed from $R=0$ upward, for *molecular* ions a certain inner region had to be excluded from the summation, to obtain a good fit. This is seen as an indication, that in-

side this region the molecules were fragmented and therefore not detected as such. The radial extension of this region is characterized by a "fragmentation radius" R_f, which may be used as a free parameter. It is expected that this radius varies monotonously with the specific energy loss.

The separation energy U may be used as a further free parameter to account, for instance, for the additional energy required to detach a proton in the formation of the $[M-\mathrm{H}]^-$ ion, and also to take care of possible Coulomb attraction and repulsion effects.

VI. COMPARISON WITH EXPERIMENTAL DATA

The model calculations were performed with the values for κ, C_v, and ρ given in Table I. It should be noted that the C_p value (specific heat at constant pressure) measured for L-valine[11] was used instead of C_v both for L- and DL-valine. This is justified since it is known (see Ref. 12) that C_v values and C_p values are very similar for these materials. The heat conductivity κ used is that of cellulose, which is known to be comparable with κ values of a number of organic compounds similar to valine (see Ref. 13). The actual κ value for valine is not known. The C_v and κ values were assumed to be temperature independent to simplify the calculations. In fact the actual values do not change significantly in the temperature range between room temperature and melting-point temperature.[14]

For the fragmentation radius and the hot core radius we chose $R_f=R_c=10$ Å (dashed curve in Fig. 5) and $R_c=R_f=30$ Å (lower solid curve in Fig. 5). Both calculations already reproduce the general trend of the data. A calculation with an energy-loss-dependent fragmentation radius R_f and $R_c=10$ Å improved the agreement significantly. The dE/dx dependence of R_f was chosen to be

$$R_f=10\ \text{Å}+0.25\ \text{Å}(dE/dx)\ , \tag{3}$$

where (dE/dx) has to be taken in units of $\mathrm{MeV/mg\,cm^{-2}}$.

A. Positive secondary ions

1. L-valine

In the calculations we used the sublimation energy of L-valine ($E_s=1.69$ eV, Ref. 15) as effective binding energy U. In Ref. 6 it is shown that this is an appropriate choice.

With $R_c=10$ Å and the energy-loss-dependent values for R_f of Eq. (3) the data for medium- and high-energy losses are rather well reproduced, while the calculated curve lies below the measured data at small dE/dx values (solid line in Fig. 4). To correct for this we tried a variation of the effective separation energy U based on the following reasoning: The high positive charge density in the cylinder around the primary-ion track will slightly reduce the separation energy U for positive secondary ions. This effect is expected to be more pronounced in the neighborhood of the track, i.e., for small distances from the track. As for increasing energy losses the radius of the area contributing to the desorption process will increase, it follows that a decreasing fraction of desorption events will be under the influence of the reduced U.

With a reduced value of $U=1.19$ eV for radii below 30 Å and $U=1.69$ for larger radii, one obtains an energy dependence which gives indeed a good fit over the whole range (dashed curve in Fig. 4). This may be indicative that the described effect may be real.

2. DL-valine

For the calculations we used the sublimation energy of L-valine, which is suggested by the results of Ref. 6. A core radius $R_c=10$ Å and the energy-loss-dependent fragmentation radius R_f of Eq. (3) yielded already sufficiently good data (see Fig. 5), so that a variation of U was not esteemed to be necessary in this case. For comparison we show in Fig. 5 plots calculated with $R_c=R_f=30$ Å and with $R_c=R_f=10$ Å.

B. Negative secondary ions

In order to reproduce the general trend of the yield data for the $[M-\mathrm{H}]^-$ secondary ions by means of the model calculations one has to use a U value which is roughly 2 eV larger than that used for $[M+\mathrm{H}]^+$ ions. An increase of the separation energy U compared to the $[M+\mathrm{H}]^+$ case is justified since an additional amount of energy is needed to separate the proton from the molecule. Here we use $U=3.69$ eV (dashed curve in Fig. 6) and $U=4$ eV (solid curve in Fig. 6) together with $R_c=10$ Å and the energy-loss-dependent fragmentation radius of Eq. (3). Both calculations reproduce the overall features of the data quite reasonably (see Fig. 6).

VII. CONCLUSION

Desorption yields for $[M+\mathrm{H}]^+$ and $[M-\mathrm{H}]^-$ secondary ions desorbed from valine samples by different primary ions are compared with the predictions of a simple macroscopic model which needs only the thermophysical properties of the sample and the effective surface binding energy as input parameters. It is possible to reproduce the data in the framework of this model using reasonable values for the core and fragmentation radii.

TABLE I. Physical parameters of valine.

Compound	ρ (g/cm^3)	C_p (J/ggrd)	Ref.	κ (J/cmsgrd)	Ref.
L-valine	1.23	1.45 (25 °C)	5	2×10^{-4} (30 °C)	13
DL-valine	1.32				

There have been a number of papers (Refs. 16–18) which describe the desorption process in a much more detailed manner by microscopic models, with more adjustable parameters. The most recent one by Lucchese[19] also incorporates a fragmentation radius.

One may say that the much simpler macroscopic model reproduces the experimental data obtained in the present paper in a similar way. These data are, on the other hand, more detailed than, e.g., those of Hedin which are used by Lucchese for comparison with his model.

The range below 10 MeV/mg cm^2 is not covered by Lucchese; also there are no data in this range given by Hedin. It would therefore be of great interest whether the microscopic models are able to reproduce these data as well as the macroscopic model does.

ACKNOWLEDGMENT

This work was supported by the Bundesministerium für Forschung und Technologie, Bonn, Federal Republic of Germany.

[1]R. D. Macfarlane and D. F. Torgerson, Science **191**, 320 (1976).

[2]See, e.g., Proceedings of the Symposium on Particle Induced Desorption and Mass Spectroscopy [J. Mass Spectrom. Ion Phys. **53**, 1 (1983)].

[3]B. Nees, E. Nieschler, N. Bischof, P. Dück, H. Fröhlich, W. Tiereth, and H. Voit, Radiat. Eff. **77**, 89 (1983).

[4]B. Nees, E. Nieschler, N. Bischof, H. Fröhlich, K. Riemer, W. Tiereth, and H. Voit, Surf. Sci. **145**, 197 (1984).

[5]P. Dück, W. Treu, H. Fröhlich, W. Galster, and H. Voit, Surf. Sci. **95**, 603 (1980).

[6]E. Nieschler, B. Nees, H. Voit, P. Beining, and J. Scheer, Phys. Rev. B **37**, 9197 (1988).

[7]C. J. McNeal, R. D. Macfarlane, and E. L. Thurston, Anal. Chem. **51**, 2036 (1979).

[8]L. C. Northcliffe and R. F. Schilling, Nucl. Data Tables **A7**, 273 (1970).

[9]P. Dück, Ph.D. thesis, University of Erlangen, 1980 (unpublished).

[10]A. Mozumder, Adv. Radiat. Chem. **1**, 1 (1969).

[11]J. O. Hutchens, A. G. Cole, and J. W. Stout, J. Phys. Chem. **67**, 1128 (1963).

[12]F. Reif, *Fundamentals of Statistical and Thermal Physics* (McGraw-Hill, Kogakusha, Tokyo, 1965).

[13]*American Institute of Physics Handbook*, 2nd ed, edited by Dwight E. Gray (McGraw-Hill, New York, 1963).

[14]*Thermophysical Properties of Matter*, edited by Y. S. Touloukian (Plenum, New York, 1970).

[15]H. J. Svec and D. D. Clyde, J. Chem. Eng. Data **10**, 151 (1965).

[16]B. V. King *et al.*, J. Chem. Phys. **82**, 3641 (1985).

[17]F. R. Krüger, Surf. Sci. **86**, 246 (1979).

[18]A. Hedin *et al.*, Phys. Rev. B **31**, 1780 (1986).

[19]R. R. Lucchese, J. Chem. Phys. **86**, 443 (1987).